nature nanotechnology

LETTERS

PUBLISHED ONLINE: XX XX 2012 | DOI: 10.1038/NNANO.2012.134

Imaging the electrocatalytic activity of single nanoparticles

Xiaonan Shan[1,2], Ismael Díez-Pérez[1,3], Luojia Wang[4], Peter Wiktor[1], Ying Gu[4]*, Lihua Zhang[1], Wei Wang[1], Jin Lu[1,5], Shaopeng Wang[1], Qihuang Gong[4], Jinghong Li[5]* and Nongjian Tao[1,2]*

The electrocatalytic properties of nanoparticles depend on their size, shape and composition[1,2]. These properties are typically probed by measuring the total electrocatalytic reaction current of a large number of nanoparticles, but this approach is time-consuming and can only measure the average catalytic activity of the nanoparticles under study. However, the identification of new catalysts requires the ability to rapidly measure the properties of nanoparticles synthesized under various conditions and, ideally, to measure the electrocatalytic activity of individual nanoparticles. Here, we show that a plasmonic-based electrochemical current-imaging technique[3] can simultaneously image and quantify the electrocatalytic reactions of an array of 1.6×10^5 platinum nanoparticles printed on an electrode surface, which could facilitate high-throughput screening of the catalytic activities of nanoparticles. We also show that the approach can be used to image the electrocatalytic reaction current and measure the cyclic voltammograms of single nanoparticles.

Scanning electrochemical microscopy (SECM) can be used to rapidly screen the electrocatalytic of nanoparticles[4]. However, SECM relies on mechanical scanning of a microelectrode across a sample surface, which limits the imaging speed and can interfere with the electrocatalytic reactions of the nanoparticles[5]. Methods that can probe the catalytic reactions of individual nanoparticles have also been developed[6–9], including nanoelectrodes[8] and super-resolution fluorescence microscopy[9]. In particular, ultramicroelectrodes have been used to monitor current spikes associated with individual collision events of nanoparticles dissolved in an electrolyte[6,7]. However, this non-imaging method cannot assign spikes to a specific nanoparticle and it is difficult to measure the entire cyclic voltammogram (CV) of each nanoparticle.

Unlike conventional electrochemical techniques (including SECM), which measure the electrical current associated with chemical reactions taking place on an electrode surface, our plasmonic-based electrochemical current imaging (P-ECi) approach measures the conversion between oxidized and reduced species near the electrode[3,10–12]. We have shown[3] that the plasmonic signal in P-ECi is directly related to the electrical current, allowing us to determine the current optically and to image the local current density of the entire electrode surface quickly (microsecond to millisecond) and non-invasively. This capability allows us to image and measure the electrocatalytic current of multiple individual nanoparticles versus time or potential, simultaneously.

Platinum nanoparticles are well known for their electrocatalytic activities. An important example is the electrocatalytic reduction of protons to generate hydrogen. To demonstrate the capability of P-ECi for high-throughput screening of the electrocatalytic reactions of platinum nanoparticles, we synthesized nanoparticles and printed them into a microarray on a gold thin-film electrode. The electrocatalytic reaction of the entire array was carried out in 0.5 M H_2SO_4 solution by scanning the potential of the gold electrode from +0.3 V to −0.53 V (versus Ag/AgCl). At negative potentials, protons in the solution are reduced to hydrogen, forming dihydrogen. The reduction process decreases the refractive index near the electrode surface, which changes the surface plasmon resonance (SPR) signal and allows us to image the local electrochemical current of the platinum nanoparticle microarrays as a function of applied potential.

Using P-ECi, we have recorded videos showing the electrocatalytic reduction current of the microarray during repeated cycling of the potential (see Supplementary Section S5 for details). One such video for a microarray of 5 nm platinum nanoparticles is presented in Supplementary Section S6 and Movie S1, and provides detailed information about the electrocatalytic reaction of each spot in the microarray. Figure 1a–f presents several snapshots of the video at different potentials. At 0.3 V (Fig. 1a), the current density is close to zero everywhere on the electrode, and the entire electrode surface is uniform, showing no contrast of the printed platinum nanoparticle microarray. As the potential is scanned to more negative values, the individual spots in the microarray begin to show up (for example, Fig. 1b). The image contrast is negative, corresponding to negative current, which is expected as a result of the electrocatalytic reduction of protons. In contrast, the current in the surrounding regions remains close to zero. The diameter of each spot is ~200 μm, but P-ECi has a spatial resolution of a few micrometres in the present set-up, so high-density microarrays can be screened and studied with the technique. By lowering the potential to −0.53 V, for example, the magnitude of the electrocatalytic current density increases in the platinum nanoparticle spots, while the current density outside the spots remains small, leading to a large negative contrast (Fig. 1c). When scanning the potential positively, the image contrast of the microarray decreases again as the electrocatalytic reaction decreases (for example, Fig. 1d). On increasing the potential to −0.3 V (Fig. 1e), the image shows a small positive contrast, which is due to the re-oxidation of hydrogen. Finally, scanning the potential back to 0.3 V, the image contrast diminishes (Fig. 1f) as the electrocatalytic reaction halts.

It is clear that P-ECi can image the electrocatalytic reaction of the entire electrode simultaneously, which is ideal for high-throughput screening of the catalytic activities of nanoparticles. The current densities are not identical for different spots in the nanoparticle microarray because of variability in the printing density of platinum

[1]Center for Bioelectronics and Biosensors, Biodesign Institute, Arizona State University, Tempe, Arizona 85287, United States, [2]School of Electrical, Computer and Energy Engineering, Arizona State University, Tempe, Arizona 85287, USA, [3]Department of Physical Chemistry, University of Barcelona, Barcelona 08028, Spain, [4]State Key Laboratory for Mesoscopic Physics, Department of Physics, Peking University, Beijing 100871, China, [5]Department of Chemistry, Tsinghua University, Beijing 100084, China. *e-mail:

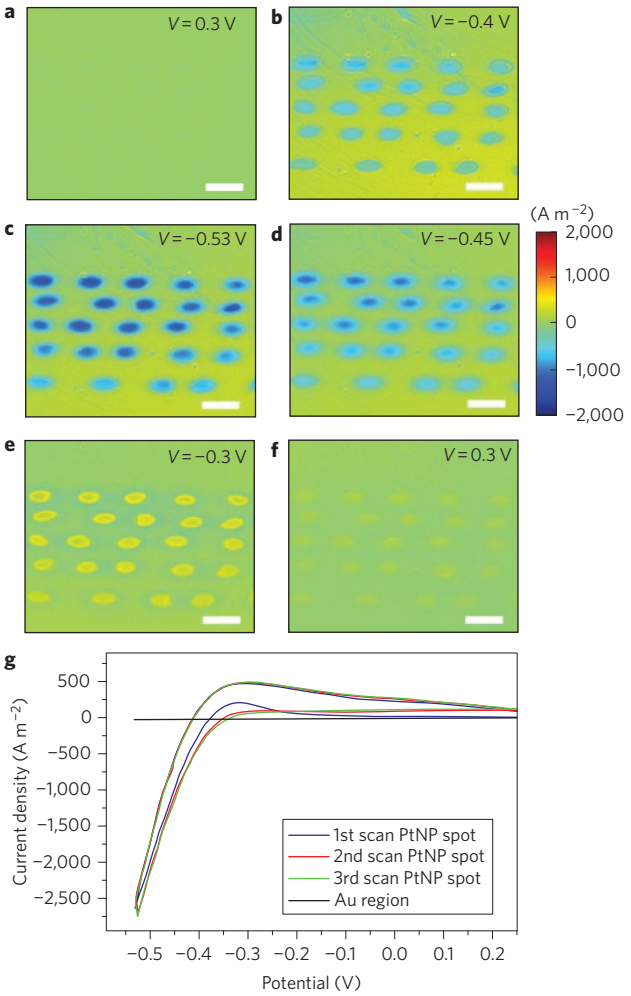

Figure 1 | P-ECi current image of a platinum nanoparticle microarray. a–f, P-ECi current density images of the platinum nanoparticle microarray at 0.3, −0.4, −0.53, −0.45, −0.3 and 0.3 V, respectively. Scale bars, 300 μm. **g**, CVs obtained by P-ECi from a single spot of the platinum nanoparticle microarray and from a bare gold region. For comparison, see Supplementary Fig. S1 for a CV of the entire surface but measured using the conventional method.

nanoparticles. For example, as shown in Fig. 1c, the spot at the upper left has a larger contrast than the one at the lower right of the microarray. Additionally, P-ECi provides quantitative information about the electrocatalytic activities of the individual nanoparticle spots in the microarray. Figure 1g presents CVs from one of the nanoparticle spots in the microarray. Compared to the CV measured using the conventional electrochemical method (Supplementary Fig. S1), the local CVs obtained by P-ECi have a similar shape but detect much higher current densities. This is because the conventional method measures the current averaged over the entire surface, including regions with and without platinum nanoparticles. To explore this, a P-ECi CV of a bare gold area is also plotted in Fig. 1g (black curve). Because of the catalytic effect of the platinum nanoparticle, the current for the platinum nanoparticle microarray is much greater than that for the bare gold area.

The capability of P-ECi in the quantitative analysis of local electrocatalytic reactions allows us to screen the nanoparticle microarrays printed onto the electrode under different conditions. To demonstrate this, we created a microarray of platinum nanoparticle spots with various surface densities of platinum nanoparticles, using printing solutions containing different concentrations of nanoparticles. The variation in microarray surface density is shown in Fig. 2a, with the nanoparticle concentration diluted by a factor of 2, column by column, from left to right. Figure 2b presents an SPR image and Fig. 2c the corresponding electrocatalytic current density image of the platinum nanoparticle microarray at −0.5 V. It is difficult to visualize the platinum nanoparticle microarrays in the SPR images, especially those with low nanoparticle surface densities (last two columns). However, P-ECi can easily resolve all the spots in the microarray because of the large electrocatalytic current at negative potentials. This observation is useful by itself, because it offers a way to enhance the imaging contrast of small nanoparticles. Orrit and colleagues[13,14] have shown that local heating of nanoparticles changes the refractive index of the surrounding medium, leading to enhanced image contrast of the nanoparticles. The present work demonstrates an alternative method to also enhance the optical image contrast.

From the P-ECi images, we obtained CVs from spots in individual columns with different nanoparticle surface densities (Fig. 2d). The CVs show similar shapes, but the electrocatalytic current at a given potential increases proportionally with nanoparticle density. We also constructed histograms of the electrocatalytic reduction current at −0.5 V (Fig. 2e), which show the dependence of the catalytic current on the surface density of platinum nanoparticles, and the variability in catalytic current for different spots with the same surface density.

Having shown that P-ECi is capable of fast and quantitative screening of the electrocatalytic properties of nanoparticles in a microarray format, we then turned to the imaging of single-nanoparticle electrocatalytic current. Figure 3a,b presents the SPR images of platinum nanoparticles with 80 nm and 40 nm diameters, respectively, where the long tails pointing in the direction of the surface plasmonic wave are due to the scattering of the plasmonic waves by nanoparticles (Supplementary Section S2). The tail shape shows little dependence on the size of the nanoparticle, but its image contrast increases with size. This result is reasonable, because the nanoparticle is much smaller than the wavelength of the plasmonic wave, such that it acts as a point scatterer with its scattering strength increasing with nanoparticle size. We simulated single-nanoparticle plasmonic images by calculating the local near-field electric field associated with the scattering of each nanoparticle. Details of the simulation are described in the Methods. The simulated images for 80 nm and 40 nm platinum nanoparticles are shown in Fig. 3d,e, which are in excellent agreement with the corresponding experimental images in Fig. 3a,b.

We imaged the electrocatalytic current of single platinum nanoparticles by cycling the elecrode potential between −0.05 V and −0.5 V. A P-ECi video showing the CV of a single nanoparticle is given in Supplementary Section S7 and Movie S2. Figure 4a–f presents a few snapshots of the video at different potentials. At −0.05 V, no electrocatalytic reaction takes place and the current is zero everywhere (Fig. 4a). Decreasing the potential to −0.36 V, the image begins to show contrast near the centre of the frame, where a nanoparticle is located. The image contrast is negative, as expected for a reduction process. The contrast increases as the potential decreases, and reaches a maximum at the lowest potential, −0.5 V (Fig. 4b–d). Sweeping the potential positively, the contrast decreases and eventually disappears, as the electrocatalytic reduction of protons diminishes at positive potentials (Fig. 4e,f). It is interesting to note the electrocatalytic current image of a single platinum nanoparticle has the same pattern as that of the regular plasmonic image, including the long tail. This is because the pattern is produced by the scattering (or diffraction) of the platinum nanoparticle, which represents the diffraction limit of P-ECi, and it does not reflect the actual geometric distribution of the current density.

To compare the P-ECi of single platinum nanoparticles with conventional electrochemical methods that measure current,

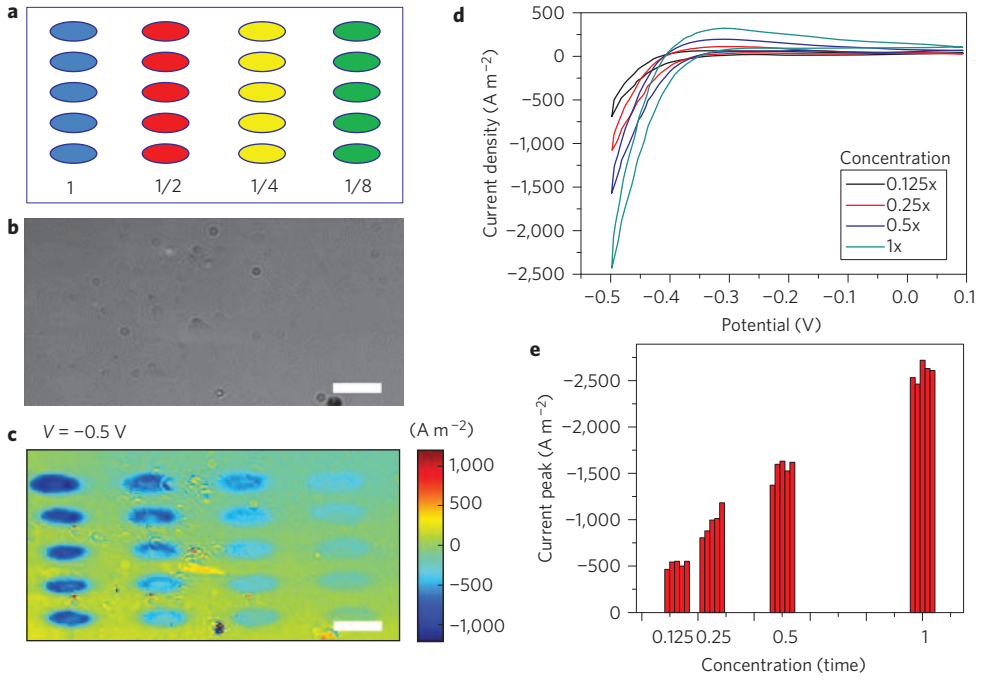

Figure 2 | Platinum nanoparticle microarray with different surface densities. a, Schematic of platinum nanoparticle spots with different surface densities. **b**, SPR image of the microarray, in which the platinum nanoparticle spots printed on the surface cannot be resolved. **c**, P-ECi image of the microarray at $V = -0.5$ V. **d**, CVs obtained by P-ECi from spots at the four different surface densities shown in **a**. **e**, Current density distribution of different spots at $V = -0.5$ V. Scale bars (**b**,**c**), 150 μm.

rather than current density, we determined the total electrocatalytic current of the single platinum nanoparticle by integrating the region of the scattering pattern (including the tail). The details are described in Supplementary Section S5. The CVs for the single nanoparticle are displayed in Fig. 4g, which shows a maximum current of ~5 nA at −0.5 V. From the noise level (~20 pA), the estimated detection limit is ~60 pA (three times the noise level), which is close to the steady-state current (40–80 pA) generated by an irreversible collision of 4 nm platinum nanoparticles reported by Bard and colleagues[6,7].

The current images shown in Fig. 4a–f were obtained using the formalism developed in ref. 3 (Supplementary Section S5). The essence of the formalism is that the plasmonic signal is related to the local concentration of reaction species[3]. To validate this basic assumption for a single nanoparticle whose plasmonic image has a long scattering tail, we measured and simulated the concentration

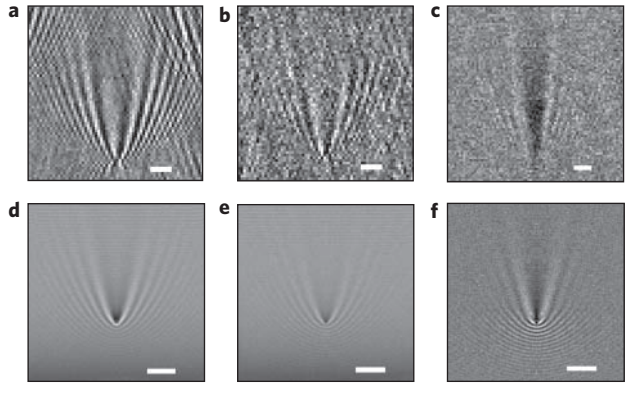

Figure 3 | Experimental and simulated SPR images of platinum nanoparticles. a,**b**, SPR images of 80 nm (**a**) and 40 nm (**b**) platinum nanoparticle after subtraction of background interference. **c**, SPR response due to electrocatalytic reaction at a potential of −0.45 V. **d**,**e**, Calculated near-field distributions of 80 nm (**d**) and 40 nm (**e**) platinum nanoparticles. **f**, Simulated SPR response of the electrocatalytic reaction that generates hydrogen around a 80 nm platinum nanoparticle. Scale bars, 2 μm.

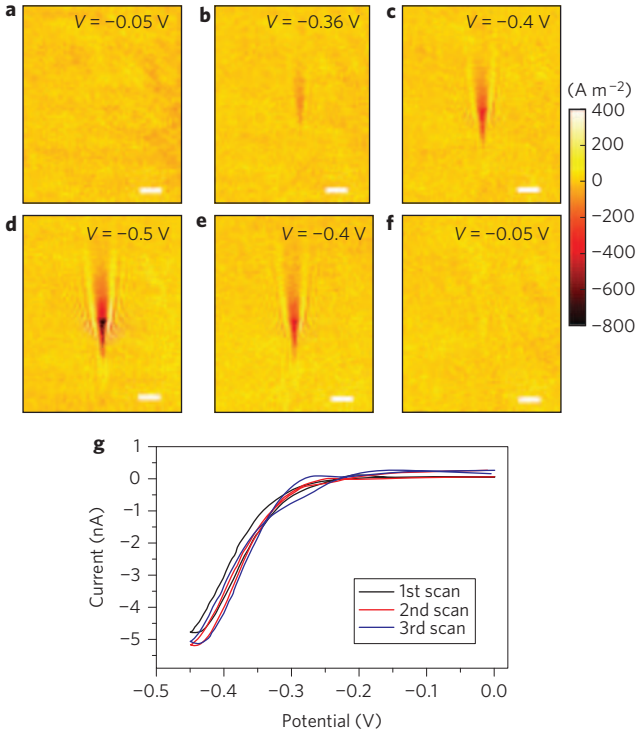

Figure 4 | Electrocatalytic reaction of a single platinum nanoparticle. a–**f**, P-ECi current density image of a single platinum nanoparticle at potentials of −0.05, −0.36, −0.4, −0.5, −0.4 and −0.05 V, respectively. Scale bars, 3 μm. **g**, CV of the single platinum nanoparticle obtained by integrating the current density over the scattering pattern, including the tail.

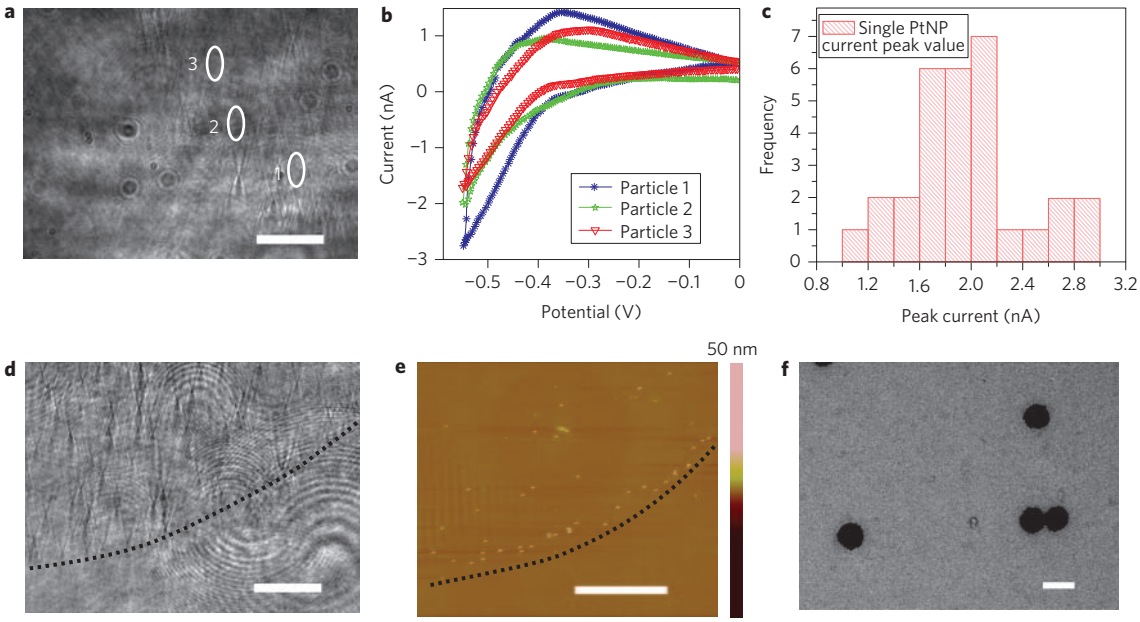

Figure 5 | Statistical analysis of single platinum nanoparticle electrocatalysis. a, SPR image of an 80 nm platinum nanoparticle microarray. **b**, CV plots of three platinum nanoparticles (locations marked in **a**). **c**, Histogram of the electrocatalytic current at a potential of −0.55 V for 30 single platinum nanoparticles, showing the large variability. **d,e**, SPR and AFM images near the edges of an 80 nm platinum nanoparticle spot. Scale bars (**a**,**d**,**e**), 15 μm. **f**, TEM images of 80 nm platinum nanoparticles. Scale bar, 100 nm.

effect on the plasmonic images. The measured effect, as shown in Fig. 3c, was determined by subtracting the image of a nanoparticle at −0.05 V from that at −0.45 V. At −0.05 V, no hydrogen is generated, so the image is entirely due to the nanoparticle. In contrast, the image at −0.45 V contains contributions from both the nanoparticle and the hydrogen generated by the electrocatalytic reaction. The simulated concentration effect was obtained by subtracting the image of a bare platinum nanoparticle from the image of the platinum nanoparticle with a thin layer (several tens to a hundred nanometres) of hydrogen-rich medium (Fig. 3f). The measured and calculated results are in excellent agreement, thus validating that the basic assumption of the formalism holds, at least approximately, even at the single nanoparticle level. This conclusion is further confirmed by the observation that the CVs of single platinum nanoparticles obtained with the formalism developed in ref. 3 are in excellent agreement with the CVs measured with the conventional electrochemcial method (Supplementary Fig. S1).

In contrast to the method that measures nanoparticle collision events by detecting transient electrocatalytic current with a microelectrode[6,7], the present approach can not only measure the CV of a single nanoparticle, but can also simultaneously study multiple nanoparticles on a surface. This latter capability makes it possible to study individual nanoparticles and measure statistics regarding their electrocatalytic properties. Figure 5a presents an SPR image of platinum nanoparticles, and Fig. 5b plots the corresponding CVs of the same platinum nanoparticles, which are marked by circles in Fig. 5a. Although the overall shapes of the CVs are similar for the different nanoparticles, the current magnitudes differ. To evaluate the variability in the electrocatalytic activity of different platinum nanoparticles, a histogram was plotted showing the distribution of electrocatalytic reduction current at −0.55 V (Fig. 5c). The large variability demonstrates the need for single-nanoparticle electrocatalytic characterization.

We characterized the platinum nanoparticle samples with SPR microscopy, atomic force microscopy (AFM) and transmission electron microscopy (TEM), giving the results shown in Fig. 5d–f. Additional images and line profiles of the platinum nanoparticle obtained from AFM and TEM are given in Supplementary Section S3.1 and Fig. S4. These high-resolution imaging techniques verify single-nanoparticle imaging by P-ECi. From the SPR images, we constructed a size distribution histogram of the platinum nanoparticles (Supplementary Section S3.2). The size distribution is relatively narrow (~10%), which further indicates that aggregation is negligible.

In summary, we have demonstrated a plasmonic method to image the electrocatalytic current of a microarray of nanoparticles and a single nanoparticle. The method is rapid, non-invasive and quantitative, making it uniquely suited for the rapid screening of the catalytic activities of nanoparticles prepared under different conditions. Because electrochemical reactions are associated with changes in the electronic states of species, which are almost always accompanied by changes in optical properties (refractive index), this method is expected to be general and suitable for the study of other electrocatalytic reactions.

Methods

Nanoparticle synthesis and characterization. Citrate-stabilized platinum nanoparticles were synthesized using a procedure reported in the literature[15]. Briefly, 1 ml of 1% H_2PtCl_6 aqueous solution was added to 100 ml of deionized water and heated to boiling point. A volume of 3 ml of 1% sodium citrate aqueous solution was quickly added into the boiling solution. The mixture was kept boiling for 30 min until the solution turned dark[15]. AFM and TEM were used to characterize the size of the synthesized platinum nanoparticles.

Nanoparticle microarray preparation. All the P-ECi experiments described here used 47-nm-thick gold films thermally evaporated onto microscope cover slides with 1.6 nm chromium adhesion layers in high vacuum (3×10^{-6} torr). Before each experiment, a gold film was annealed with a H_2 flame for 10 s to remove possible contaminations. The flame-annealed gold film was then immediately soaked in a 1 mM 1,3-propanedithiol ethanol solution for ~8 h. The dithiol layer helped immobilize the platinum nanoparticles on the surface. Different concentrations of platinum nanoparticle solutions were printed onto the gold film with a piezoelectric microprinter to form a microarray of platinum nanoparticle spots with various nanoparticle surface densities. The spot size was controlled in the range 50–350 μm. After printing, the surface was allowed to dry and then rinsed with deionized water for 10 s to remove salt residues from the platinum nanoparticle solutions and unbound nanoparticles. After drying with N_2 gas, the nanoparticle microarray was mounted onto the P-ECi set-up with a Teflon electrochemical cell.

Electrochemical measurement. The Teflon electrochemical cell mentioned above was filled with 0.5 M H_2SO_4 solution. The gold film served as the working electrode

and a platinum wire as the counter-electrode. The potential of the gold film was controlled with respect to either a silver wire quasi-reference electrode or Ag/AgCl reference electrode with an Autolab potentiostat.

Optical set-up and data analysis. The P-ECi experiments were performed using two set-ups—prism-based and microscope-based[16,17]—to cover both low- and high-spatial-resolution imaging needs for the microarray and single nanoparticle studies. In the prism set-up, p-polarized light from a 670 nm light-emitting diode (LED) was directed through a prism onto the gold film placed on the prism. The reflected beam produced an SPR image, which was captured by a Pike camera and converted into an electrochemical current image using the formalism described in Supplementary Section S5 (ref. 3). The microscope set-up was based on an inverted total internal reflection fluorescence image set-up[18]. The prism-based set-up had a large view (but limited spatial resolution), and was used for microarray studies. The microscope-based set-up, in contrast, had a small view but high spatial resolution, and was used to image single-nanoparticle electrocatalytic reactions.The light source used for the microscope set-up was a 1 mW super LED (wavelength, 680 nm). The power at the sample surface was reduced to ~30 μW after passing through a polarizer, beamsplitters and other optical components. Note that to remove background interference in the SPR images (for example, Fig. 3a,b), the substrate was moved laterally by 500 nm; one image was captured before the lateral movement, and one after. Subtracting one image from the other removed the background interference patterns.

Numerical simulation. Three-dimensional numerical simulations of the nanoparticle SPR images were performed with the radiofrequency module of COMSOL multiphysics software. Surface plasmons at the interface between a gold film and water were excited by a p-polarized incident plane wave (wavelength, 680 nm), and a platinum nanoparticle located above the gold film served as a scatterer. The dimensions of the gold film were 16 μm × 12 μm × 47 nm, which was set to be periodic to produce uniform simulations. The refractive indices used in the simulations were 1.51391, 1.331, 0.16146 + 3.6420i and 2.47848 + 4.3888i for glass, water, gold and platinum, respectively. The asymmetric three-layer planar structure (glass, gold film and water) supported two surface modes as a result of mode coupling, and the indices of two modes were found to be 1.7043 and 1.4283, respectively, according to the two-dimensional dispersion relation[19]. The latter mode has a longer propagation length and stronger fields on the water side, which was the central focus of the simulations. The three-dimensional simulations were carried out by varying the incident angle from 68.6° to 73.7°, and the result showed that the reflection reached a minimum at 70.6°, which corresponds to the excitation of the long-range mode with a surface plasmon wavelength of 476 nm (ref. 14). The scattering of the long-range mode by the nanoparticle was simulated with an incident angle of 70°. The scattering pattern featured stripes ~230 nm wide, corresponding to the half-wavelength of the surface plasmons[20].

Received 4 May 2012; accepted 12 July 2012; published online XX XX 2012

References

1. Zhou, Z. Y., Tian, N., Li, J. T., Broadwell, I. & Sun, S. G. Nanomaterials of high surface energy with exceptional properties in catalysis and energy storage. *Chem. Soc. Rev.* **40,** 4167–4185 (2011).
2. Shan, X. N. *et al.* Measuring surface charge density and particle height using surface plasmon resonance technique. *Anal. Chem.* **82,** 234–240 (2010).
3. Shan, X. N., Patel, U., Wang, S. P., Iglesias, R. & Tao, N. J. Imaging local electrochemical current via surface plasmon resonance. *Science* **327,** 1363–1366 (2010).
4. Bard, A. J. *et al.* Chemical imaging of surfaces with the scanning electrochemical microscope. *Science* **254,** 68–74 (1991).
5. Lu, X., Wang, Q. & Liu, X. Review: recent applications of scanning electrochemical microscopy to the study of charge transfer kinetics. *Anal. Chim. Acta* **601,** 10–25 (2007).
6. Xiao, X. Y. & Bard, A. J. Observing single nanoparticle collisions at an ultramicroelectrode by electrocatalytic amplification. *J. Am. Chem. Soc.* **129,** 9610–9612 (2007).
7. Xiao, X. Y., Fan, F. R. F., Zhou, J. P. & Bard, A. J. Current transients in single nanoparticle collision events. *J. Am. Chem. Soc.* **130,** 16669–16677 (2008).
8. Li, Y. X., Cox, J. T. & Zhang, B. Electrochemical responses and electrocatalysis at single Au nanoparticles. *J. Am. Chem. Soc.* **132,** 3047–3054 (2010).
9. Zhou, X. *et al.* Quantitative super-resolution imaging uncovers reactivity patterns on single nanocatalysts. *Nature Nanotech.* **7,** 237–241 (2012).
10. Foley, K. J., Shan, X. & Tao, N. J. Surface impedance imaging technique. *Anal. Chem.* **80,** 5146–5151 (2008).
11. Shan, X. N., Wang, S. P., Wang, W. & Tao, N. J. Plasmonic-based imaging of local square wave voltammetry. *Anal. Chem.* **83,** 7394–7399 (2011).
12. Wang, S. P., Huang, X. P., Shan, X. N., Foley, K. J. & Tao, N. J. Electrochemical surface plasmon resonance: basic formalism and experimental validation. *Anal. Chem.* **82,** 935–941 (2010).
13. Boyer, D., Tamarat, P., Maali, A., Lounis, B. & Orrit, M. Photothermal imaging of nanometer-sized metal particles among scatterers. *Science* **297,** 1160–1163 (2002).
14. Gaiduk, A., Yorulmaz, M., Ruijgrok, P. V. & Orrit, M. Room-temperature detection of a single molecule's absorption by photothermal contrast. *Science* **330,** 353–356 (2010).
15. Huang, M. H. *et al.* Alternate assemblies of platinum nanoparticles and metalloporphyrins as tunable electrocatalysts for dioxygen reduction. *Langmuir* **21,** 323–329 (2005).
16. Rothenhausler, B. & Knoll, W. Surface-plasmon microscopy. *Nature* **332,** 615–617 (1988).
17. Huang, B., Yu, F. & Zare, R. N. Surface plasmon resonance imaging using a high numerical aperture microscope objective. *Anal. Chem.* **79,** 2979–2983 (2007).
18. Wang, S. *et al.* Label-free imaging, detection, and mass measurement of single viruses by surface plasmon resonance. *Proc. Natl Acad. Sci. USA* **107,** 16028–16032 (2010).
19. Wang, L., Gu, Y., Hu, X. & Gong, Q. Long-range surface plasmon polariton modes with a large field localized in a nanoscale gap. *Appl. Phys. B* **104,** 919–924 (2011).
20. Zayats, A. V., Smolyaninov, I. I. & Maradudin, A. A. Nano-optics of surface plasmon polaritons. *Phys. Rep. Rev. Sec. Phys. Lett.* **408,** 131–314 (2005).

Acknowledgements

This work was supported by the National Science Foundation (CHE-1105588), the National Natural Science Foundation of China (no. 11121091), the National Basic Research Program of China (no. 2011CB935704) and the Natural Science Foundation of China (no. 20975060). I.D.P. thanks the Ramon y Cajal programme of the Spanish Government for funding.

Author contributions

X.N.S. carried out the experiments and analysed the experimental data. I.D.P., P.V., L.Z., W.W., J.L. and J.H.L. helped with sample preparation. S.W. helped with instrumentation. L.J.W., Y.G. and Q.H.G. carried out theoretical simulations. N.J.T. conceived the project. X.N.S. and N.J.T. wrote the paper.

Additional information

Supplementary information is available in the online version of the paper. Reprints and permission information is available online at http://www.nature.com/reprints. Correspondence and requests for materials should be addressed to Y.G., J.L. and N.T.

Competing financial interests

The authors declare no competing financial interests.

Publisher: Nature

Journal: Nature Nanotechnology

Article number: nnano.2012.134

Author (s): Xiaonan Shan *et al*.

Title of paper: Imaging the electrocatalytic activity of single nanoparticles

Query no.	Query	Response
1	Please provide correspondence email addresses	
2	Should this be “to rapidly screen the electrocatalytic activity” or “reaction”?	
3	Sentence beginning “An important” OK as amended?	
4	Sentence beginning “The image contrast” OK as amended?	
5	Sentence beginning “By lowering” OK as amended?	
6	Please check that paragraph beginning “It is clear” is OK as amended?	
7	Sentence beginning “To explore” OK as amended?	
8	Sentence beginning “The present work” OK as amended? I have shortened this to avoid repeating text in the previous sentence. Please check that this still adequately reflects your meaning.	
9	Changed to “rather than current density” – is this what you mean?	
10	Changed to formalism to agree with elsewhere – OK?	
11	Sentence beginning “In contrast” OK as amended?	
12	Sentence beginning “Figure 5a” OK as amended?	
13	Sentence beginning “The method” OK as amended?	
14	Sentence beginning “Because” OK as amended?	
15	Sentence beginning “Subtracting” OK as amended?	

16	RF expanded OK?	
17	I have made the notation consistent here by deleting the end 0 from 0.40 etc. Please check.	
18	Please confirm that 0.55 is a potential, as amended	
19	Please check that Fig 5d,e caption is OK as amended (to singular nanoparticle).	